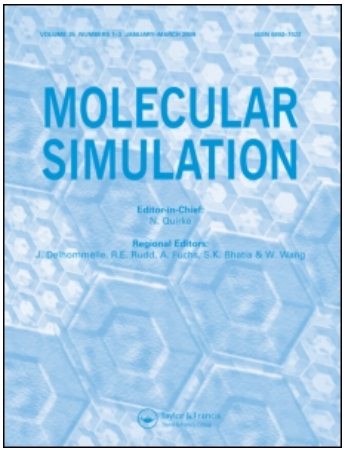

Molecular Simulation
Publication details, including instructions for authors and subscription information:
http://www.informaworld.com/smpp/title~content=t713644482

Crystallographic Refinement and Structure-Factor Time-Averaging by Molecular Dynamics in the Absence of a Physical Force Field

Piet Gros[a]; Wilfred F. Van Gunsteren[a]
[a] Laboratory of Physical Chemistry Swiss, Federal Institute of Technology (ETH) ETH-Zentrum, Zürich, Switzerland

To cite this Article Gros, Piet and Van Gunsteren, Wilfred F.(1993) 'Crystallographic Refinement and Structure-Factor Time-Averaging by Molecular Dynamics in the Absence of a Physical Force Field', Molecular Simulation, 10: 2, 377 — 395
To link to this Article: DOI: 10.1080/08927029308022174
URL: http://dx.doi.org/10.1080/08927029308022174

Molecular Simulation, 1993, Vol. 10(2-6), pp. 377-395
Reprints available directly from the publisher
Photocopying permitted by license only

CRYSTALLOGRAPHIC REFINEMENT AND STRUCTURE-FACTOR TIME-AVERAGING BY MOLECULAR DYNAMICS IN THE ABSENCE OF A PHYSICAL FORCE FIELD

PIET GROS and WILFRED F. VAN GUNSTEREN

Laboratory of Physical Chemistry
Swiss Federal Institute of Technology (ETH)
ETH-Zentrum, 8092 Zürich
Switzerland
e-mail: wfvgn@igc.ethz.ch

(Received December 1992, accepted December 1992)

The application of Molecular-Dynamics simulation in protein-crystallographic structure refinement has become common practice. In this paper, structure optimizations are described where the driving force is derived only from the crystallographic data and not from any physical potential energy function. Under this extreme condition *ab initio* structure refinement and the application of structure-factor time averaging was investigated using a small 9 atom test system. Success in *ab initio* refinement, where the starting atomic positions are randomly distributed, depends on the resolution of the crystallographic data used in the optimization. The presence of high resolution data introduces false minima in the X-ray energy profile, enhancing the search problem significantly. On the same system, we also tested the method of time-averaged crystallographically restrained Molecular Dynamics, again in the absence of a physical force field. In this method, the diffraction data is modelled by an ensemble of structures instead of one single structure. In comparison to conventional single-structure refinement, more reflections were required to determine a correct atomic distribution. A time-averaging simulation at 0.2 nm resolution (40 reflections) yielded an incorrect distribution, although a low R-factor was obtained. Simulations at 0.1 nm resolution (248 reflections) gave both low R-factors, 3 to 4%, and correct atomic distributions. The scale factor between the observed and time-averaged calculated structure factor amplitudes appeared to be unstable, when optimized during a time-averaging simulation. Tests of time-averaged restrained simulations with noise added to the observed structure-factor amplitudes, indicated that noise is modelled when no information in the form of constraints or restraints is available to distinguish it from real data.

KEY WORDS: molecular dynamics, protein crystallography, crystal structure refinement, time-averaged restrained molecular dynamics

1 INTRODUCTION

In protein crystallography and Nuclear Magnetic Resonance (NMR) structure determinations, Molecular Dynamics (MD) has been used primarily as an efficient search method in structure refinement [1, 2, 3, 4, 5, 6]. This application of MD in protein crystallography has reduced the human time spent on refining a macromolecular structure greatly compared to least-squares methods. The nature of the final refined model, however, is left unchanged. Such a refined model generally consists of a single conformation with three positional parameters and one displacement

parameter, or crystallographic temperature (B) factor, for each atom. This 'static' model poorly represents the structural variability in the crystal [see e.g. 7]. Typically the atomic probability distributions, and hence the electron density distribution are anisotropic and may have multiple maxima. Especially at high resolution these features may become important, and the data is not served well by an isotropic single-site model [8]. A description of more complicated distributions requires multiple displacement parameters. Already six parameters are required to describe Gaussian anisotropy. Unfortunately, the low observation to parameter ratio for macromolecular diffraction data does not allow fitting of much more than 3 positional parameters and one B-factor per atom. MD simulations, however, sample the configurational space of the simulated molecules, and thus provide the ensemble of possible conformations (see e.g. [9] for an overview on MD simulations). In essence, MD supplies a theoretical model for the distribution of conformations that is missing in the conventional structure refinement. The method of time-averaged restrained MD [10, 11] applies this information on atomic distributions in the modelling of the experimental data. It combines the physical, empirically derived, potential energy function and an appropriate pseudo-energy function representing the experimental data. The pseudo-energy function is chosen to penalize deviations of the calculated (time-averaged) structure-factor amplitudes from the experimentally measured amplitudes. Applying MD with this combined potential function generates an ensemble of conformations, distributed according to Boltzmann's law, that thus treats all possible distributions of the molecular system in a general fashion.

The first formulation of time-averaging was posed by Torda *et al.* [12]. They defined time-averaged NMR-Nuclear Overhauser Effect (NOE) restraints and applied it to tendamistat [10]. Their resulting ensemble model showed a larger structural flexibility than conventional MD refinement and agreed better with the experimental distance bounds. Subsequently, the technique has been applied to other NMR-NOE data sets, both experimental data sets and test data sets [13, 14, 15]. Recently, Torda *et al.* [16] extended the method to include time-averaged J-coupling constant restraints from NMR data. In the case of single-crystal X-ray diffraction data, the application of time averaging has been demonstrated by Gros *et al.* [11, 17]. This first application to diffraction data from bovine pancreatic phospholipase A2 revealed large variabilities in the loops that are involved in lipid bilayer association. The implied structural mobility is consistent with the X-ray diffraction and other biochemical data, but overlooked when using the classical single structure representation of the X-ray crystal structure. In the present paper, we discuss the application of MD in crystallographic structure refinement with and without structure-factor time averaging. We chose to perform all the computational experiments on a small 9 atom-test system in the absence of a physical force field. The potential energy function, therefore, contains only the pseudo-energy term of the diffraction data. This highlights effects of the pseudo-energy term in the calculations, that otherwise might remain obscured through the presence of other terms in the potential energy function. Conventional MD-refinement calculations starting from either correct and random atomic positions were performed testing the effects of structure-factor resolution limits. We also performed time-averaged restrained MD-simulations to test the effects of resolution limits on the data, noise present in the diffraction data, optimization of the scale factor between observed and calculated structure-factor amplitudes, and the

sampling behaviour at different structure-factor relaxation times (see Section Theory) and atomic B-factors.

2 THEORY

The standard target function in the MD refinement calculations consists of two components, see Equation (1). The first component is an empirically derived physical potential function, V_{phys} (see e.g. [18]), that models the stereochemistry and the van der Waals and electrostatic interactions. Added to this is a penalty function for fitting the experimental data, in this case the crystallographic data, $V_{X\text{-}ray}$.

$$V_{pot}(r) = V_{phys}(r) + V_{X\text{-}ray}(r) \tag{1}$$

The experiments described in this paper are performed with V_{phys} set to zero. The common expression for the pseudo-energy term $V_{X\text{-}ray}$ in structure refinement is given in Equation (2) [5, 6].

$$V_{X\text{-}ray}(r) = \frac{1}{2} k_x \sum_s (|F_{obs}(s)| - k|F_{calc}(r,s)|)^2 \tag{2}$$

where $r = \{r_1, r_2, \ldots r_N\}$ are the positional vectors of the N atoms, k_x is the crystallographic force constant, s is a reciprocal lattice vector, $|F_{obs}(s)|$ is an observed structure factor amplitude and $|F_{calc}(r,s)|$ is a structure factor amplitude computed from the atomic model. The structure-factor scaling factor k is calculated according to Fujinaga *et al.* [6].

$$k = \frac{\sum_s |F_{obs}(s)||F_{calc}(s,r)|}{\sum_s |F_{calc}(s,r)|^2} \tag{3}$$

The independent variables in Equation (2) are the three positional parameters and one isotropic temperature factor for each atom in the structural model. Equation (2) uses the instantaneous structure factors corresponding to a single structure. The model resulting from a minimization of $V_{X\text{-}ray}$ (Equation (2)) is, therefore, a single-site structure with optimized coordinates and isotropic B-factors.

For collecting an ensemble of structures Equation (2) has to be adapted slightly, see Equation (4). The instantaneous or single configuration value of the structure factor $F_{calc}(r,s)$ has to be replaced by the time-averaged or ensemble-averaged value $\langle F_{calc}(r,s)\rangle$.

$$V_{X\text{-}ray}(r) = \frac{1}{2} k_x \sum_s (|F_{obs}(s)| - k|\langle F_{calc}(r,s)\rangle|)^2 \tag{4}$$

The ensemble average of structure factors is, of course, not available when generating the ensemble. The alternative is to use a running average of the calculated structure factors. For practical reasons [12] the definition of the running average, see Equation (5), contains an exponential memory damping factor with a memory relaxation time τ_x. The standard average is obtained for infinite τ_x. In this case the contribution of instantaneous structure factors to the average values approaches

zero as time proceeds, and consequently the force derived from Equation (5) also becomes zero. Therefore, a finite τ_x must be used. As shown in Equation (5) the running average structure factors can readily be computed during the simulation.

$$\begin{aligned}\langle F_{\text{calc}}(r,s)\rangle_t &= \frac{1}{\tau_x(1-e^{-t/\tau_x})}\int_0^t e^{-(t-t')/\tau_x}F^{t'}_{\text{calc}}(r,s)\,dt' \\ &\approx e^{-\Delta t/\tau_x}\langle F_{\text{calc}}(r,s)\rangle_{t-\Delta t} + (1-e^{-\Delta t/\tau_x})F^t_{\text{calc}}(r,s)\end{aligned} \tag{5}$$

where Δt is a finite time difference between structure factor updates. To derive gradients of the time-averaged restraint with respect to coordinate positions, we followed the derivation of Agarwal [19] for obtaining gradients to Equation (4). In comparison to the gradient formula given by Agarwal, the instantaneous structure factors, $F_{\text{calc}}(r,s)$, are replaced by the running-average $\langle F_{\text{calc}}(r,s)\rangle_t$, and the phase angle, $\alpha_{\text{calc}}(s)$ is now replaced by the phase of the running-average structure factor, $\alpha_{\text{av}}(s)$ (see Equation (6), which shows the gradient with respect to the x coordinate of atom m; gradient formulas for the y and z coordinates can be derived analogously). As pointed out by Lifchitz (in [20]), the gradient can then be calculated from one difference map, D, convoluted with the derivative of the atomic electron density of atom m, ρ'_m. For the time-averaged restraint, the difference map D_{av} is the fourier transform of $(k\,|\langle F_{\text{calc}}(r,s)\rangle_t| - |F_{\text{obs}}(s)|)\exp[i\alpha_{\text{av}}(s)]$.

$$\begin{aligned}G(x_m) &= \sum_s g_m(s) \\ &\quad (-i2\pi h)[k\,|\langle F_{\text{calc}}(r,s)\rangle_t| - |F_{\text{obs}}(s)|]\,e^{i\alpha_{\text{av}}(s)}e^{-i2\pi s\cdot r_m} \\ &= D_{\text{av}}(r)\cdot\rho'_m(r)\end{aligned} \tag{6}$$

where $g_m(s)$ is the contribution of the m^{th} atom to the structure factors ($g_m(s) = f_m(s)\exp[-B_i|s|^2/4]$, where f_m is the scattering factor of atom m and B_i is the atomic temperature factor), h is the reciprocal lattice index along axis a^* (same notation has been used as in [19, 20]). In the derivation of Equation (6), we have implicitly multiplied $V_{\text{X-ray}}$ by the inverse of $(1 - e^{-\Delta t/\tau_x})$. At the conditions of interest to us, τ_x is much larger than Δt. The forementioned factor $1 - e^{-\Delta t/\tau_x}$ then has a value near zero, and the crystallographic force would become ineffective. When using Equation (6) and thus compensating the factor $(1 - e^{-\Delta t/\tau_x})$, the X-ray forces in conventional MD refinement and in structure-factor time averaging MD simulation are in the same order of magnitude.

3 METHODS

The test system consisted of 9 atoms of equal type, carbon, and with identical crystallographic temperature factors, B_i's, of 0.10 nm^2. The atoms were placed at the corners of a cube with 0.2 nm edges, with one atom occupying the center of the cube. This centrosymmetric structure was placed in an unit cell with $P_{\bar{1}}$ symmetry with edges of $a = b = c = 0.5$ nm and all angles 90°. Crystallographic data was calculated up to 0.1 nm resolution, and subsequently used as the 'observed'

structure factor amplitudes. Besides this perfect data set, a data set with ca. 10% noise in R-factor was generated by perturbing the structure factor amplitudes randomly.

In the refinements we used P_1 symmetry for the unit cell. A starting structure of 9 atoms was generated by selecting random coordinates with the constraint of minimal 0.01 nm interatomic distances. In the conventional refinement experiments (i.e. excluding time-averaging experiments) we used ideal atomic B-factors, $B_i = 0.10\,\text{nm}^2$. The number of independent parameters was, therefore, only 27 in these calculations.

The potential energy function used in all MD calculations contained only the crystallographic pseudo-energy function. This X-ray term is shown in Equation (2) for conventional refinement and in Equation (4) for structure-factor averaging. A time step of $\Delta t = 2\,\text{fs}$ was used in the simulations. The initial velocities of the 9 particles were taken from a Maxwellian distribution with $T_{t=0} = 300\,\text{K}$. The temperature was tightly coupled to a temperature bath [21] with $T_{\text{bath}} = 300\,\text{K}$ and $\tau_T = 10\,\text{fs}$. The grid spacing in the electron-density calculation was set at 0.033 nm, independent of the upper resolution limit (maximum upper resolution limit applied was 0.1 nm resolution). The structure factors and gradients were updated every time step. An appropriate value for the crystallographic weight factor, $w_x = \frac{1}{2}\ k_x$, was determined for the selected temperature by performing conventional MD refinements starting from a correct solution. A too large weight factor results in too abruptly changing forces with respect to the stepsize, and a too small weight factor renders the X-ray potential energy function ineffective. This selection of force constant ensures a proper balance between forces derived from the crystallographic pseudo-energy function with respect to the temperature and time step in the simulation. Refinements were performed with a variety of upper resolution limits in $V_{\text{X-ray}}$. No lower resolution boundary was employed, i.e. all reflections except $s = 0$ up to the upper resolution limit were taken into account.

Time-averaging MD simulations were performed starting from a correct centered cube configuration, thus $\langle F_{\text{calc}}(r, s)\rangle_{t=0} = F_{\text{calc}}(r(t = 0), s)$ which corresponds to a perfect solution with a crystallographic R-factor of 0. Two equilibration schemes were employed. In equilibration type I, τ_x and B_i were set to the requested values at $t = 0\,\text{ps}$. Equilibration type II started with $\tau_x(t = 0) = 0\,\text{ps}$ and $B_i = 0.10\,\text{nm}^2$, that were linearly increased and decreased respectively to the final τ_x value and $B_i = 0.01\,\text{nm}^2$ over a period of $t = 2\tau_x$. Scheme I was employed in the first set of time-averaging simulations. In these experiments, short simulations over a time period τ_x were performed with various combinations of τ_x and B_i (see Section Results and Discussion Table 2). In the simulations where a complete ensemble was collected with $\tau_x = 2.5$ and 5 ps, we employed scheme II. For the simulation with $\tau_x = 10\,\text{ps}$ we used the results of the run with $\tau_x = 5$ at $t = 80\,\text{ps}$ as a starting point. Ensembles were collected over 30, 50 and 100 ps after 20, 20 and 30 ps equilibration for the experiments with $\tau_x = 2.5$, 5 and 10 ps respectively with $B_i = 0.01\,\text{nm}^2$.

In our test case, the value for the structure-factor scaling factor, k, is perfectly known a priori. In realistic applications of MD refinement this is not the case. We have tested two different methods for updating this scale factor in the time-averaging simulations. Firstly, unrestrained updating of the scale factor has been applied at 10 (20 fs) and 100 (0.2 ps) step intervals, using Equation (3) with $F_{\text{calc}}(s)$ replaced by $\langle F_{\text{calc}}(s)\rangle_t$. Secondly, we tested a time-dependent update of the scale

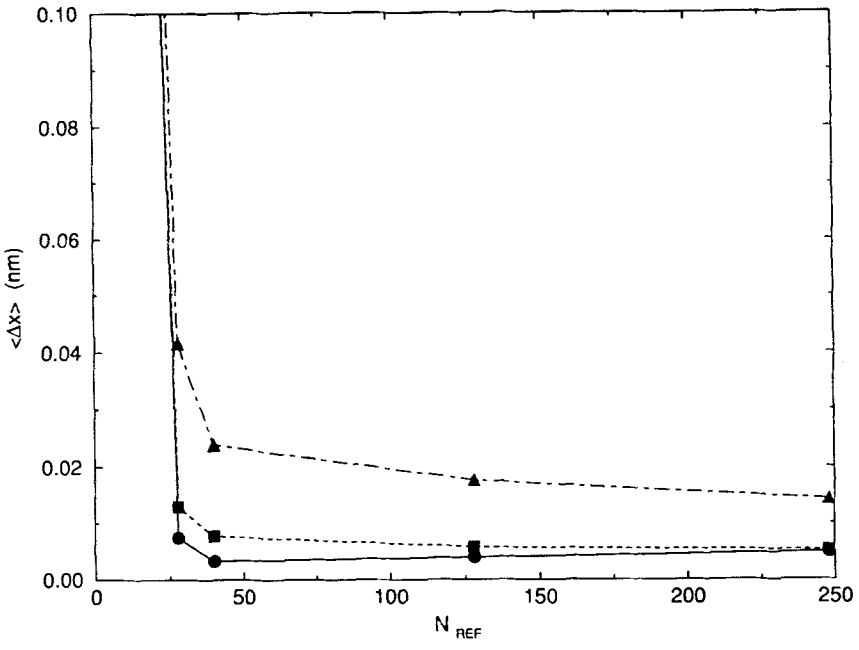

Figure 1a

factor which was applied every step, see Equation (7). Equation (7) effectively reduces the rate of change of the scale factor.

$$k = \langle k_t \rangle = \frac{1}{\tau_k} \int_0^t e^{-(t-t')/\tau_k} k_{t'} dt' \tag{7}$$

where, k_t is the instantaneous scale factor between $|\langle F_{\text{calc}} \rangle_t|$ and $|F_{\text{obs}}|$ (calculated analogous to Equation (3)), and τ_k is the scale factor relaxation time.

For all calculations we used Gromox, a crystallographic extension of the MD-simulation program of GROMOS [18]. The computations were performed on a SUN Sparc-2 workstation.

4 RESULTS AND DISCUSSION

a Stability of a correct structure as a function of resolution

The stability of the correct solution was tested with respect to various X-ray weights, $w_x = \frac{1}{2} k_x$, and different upper resolution limits of the data. A weight of 3.052 10^5 (kJ mol^{-1} I^{-1}, where I is an arbitrary unit for structure factor intensities) produced the best results. A ten-fold larger force constant resulted in abrupt changes in the forces, causing very high temperatures when data beyond 0.13 nm was used. A ten-fold reduction in X-ray weight resulted in insufficient restraining of the points to maintain a correct solution at the chosen temperature.

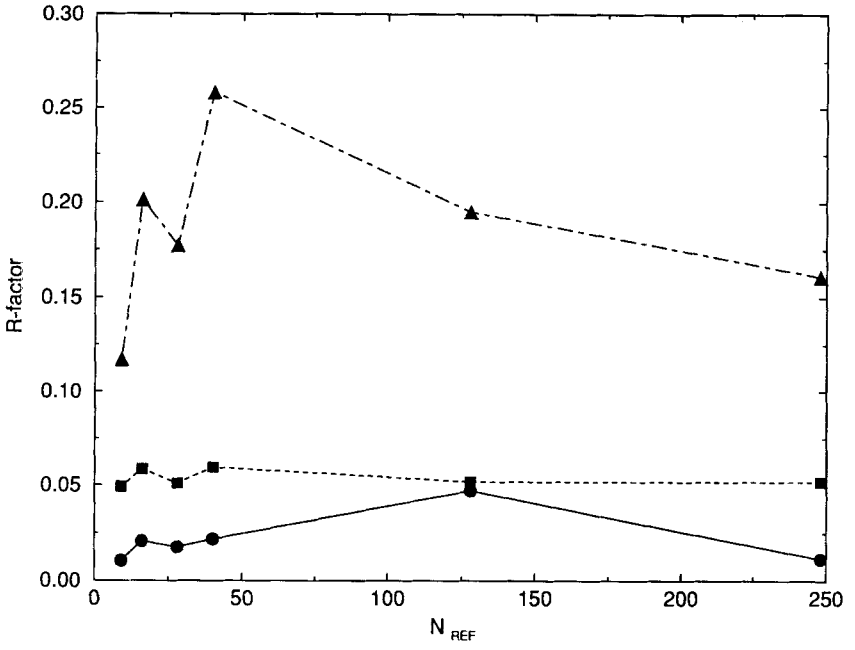

Figure 1 Stability of the correct answer in the crystallographic force field. 250 MD steps (0.5 ps) of conventional MD-refinement were carried out starting from the correct structure ($T_{t=0} = T_{bath} = 300$ K). Different upper resolution limits were tested: 0.3 nm (9 reflections), 0.25 (16 refl.), 0.22 nm (28 refl.), 0.2 nm (40 refl.), 0.125 (128 refl.) and 0.1 nm (248 refl.). (a) Coordinate deviation Δx averaged over the 9 particles is plotted as a function of the number of reflections N_{ref}; and (**b**) the crystallographic R-factor, $R = \Sigma \| F_{obs}(s) | - k | F_{calc}(s) \| / \Sigma | F_{obs}(s) |$ as a function of the number of reflections. Three different weights, w_x, were employed: 3.052 10^6 (circles connected by solid lines), 3.052 10^5 (squares and dashed lines) and 3.052 10^4 (triangles and dot-dashed lines). These weight factors account for the conversion factor from structure-factor intensity units to kJ mol^{-1}. The structure-factor intensities, and thus the amplitudes, are on an arbitrary scale. The structure-factor scaling factor was set to a value of $k = 1$.

Only 28 reflections, corresponding to data up to 0.22 nm resolution, were required to maintain the correct structure over 0.5 ps at 300 K, see Figure 1a. The average coordinate deviation was well below 0.02 nm at this resolution ($w_x = 3.052\ 10^5$). Extending the resolution to 0.2 nm (40 reflections) reduced the average coordinate deviation to less than 0.01 nm. No significant improvement was obtained by extending the data beyond 0.2 nm. Figure 1b shows that very similar R-factors were obtained at different resolution limits, showing no relationship with the actual coordinate error. When less than 0.22 nm resolution data is used, the ratio of intensities to atomic coordinates is lower than one. The system is no longer uniquely determined by the data, and, not surprisingly, large coordinate errors are observed under these conditions. A parameter to observation ratio of one is, however, already sufficient to retain a correct solution.

b Ab initio MD refinement at different resolutions

Starting from random coordinates correct centered-cube configuration could be obtained within 100 steps (0.2 ps) of MD-refinement, see Figure 2. In that

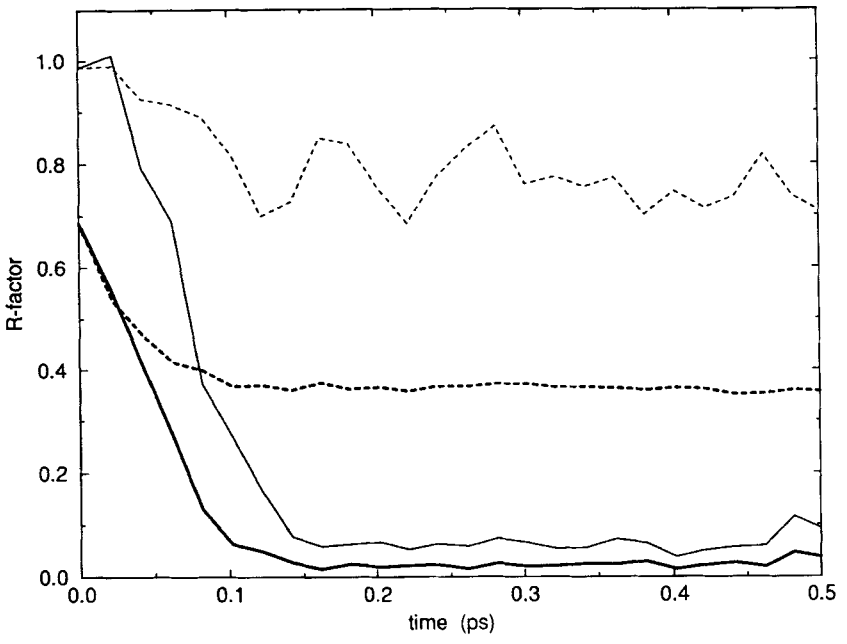

Figure 2 *Ab initio* MD refinement. Starting from random coordinates the 9 atoms were optimized against the crystallographic data only, using 0.1 nm resolution data. The crustallographic R-factor is shown as a function of the time step for all data (thick lines) and for a high resolution shell (thin lines): 0.111 to 0.100 nm resolution (54 reflections). The simulations were performed with $w_x = 3.052\ 10^5$, $k = 1$, and at constant temperature: data for $T_{t=0}$ and T_{bath} at 200 K are shown in solid lines, data for 300 K shown in dashed lines.

experiment we used data to 0.1 nm resolution, and the optimization was run at constant bath temperature of 200 K. The maximum coordinate deviation from a perfect configuration was less than 0.01 nm for the final solution. However, changing the optimization conditions slightly, using a starting temperature and bath temperature of 300 K, yielded an incorrect structure (see Table 1). This indicates the existence of local minima.

For an idealized local minimum structure "1" (see Table 1) we computed the X-ray energy and R-factor profiles for moving the two incorrectly placed atoms towards the correct positions, see Figure 3a. Data to 0.1 nm resolution created a false minimum with an energy barrier of ca. 20% of the maximum energy depicted in Figure 3a. When the resolution was reduced to 0.2 nm, this false minimum disappeared, as is shown in Figure 3b.

Two general ways of avoiding local minima in crystal structure refinement have been suggested in the literature, *i)* simulated annealing (SA) using all observed data [5, 22]; and *ii)* gradual resolution extension [23]. We tested both methods starting from the configuration at local minimum number 1 (Table 1). A small number of SA runs were performed, which got trapped in (lower) local energy minima and did not find the global energy minimum. In Figure 4 an example of a SA run is given. The local minimum, that is found there, is given in Table 1 as local minimum 2. Possibly, better results from the SA refinement could be

Table 1 Atom positions at the global minimum and at two local minima of the X-ray pseudo-energy function.

	correct centered cube		
atom number	*x (nm)*	*y (nm)*	*z (nm)*
1	0.	0.	0.
2	0.2	0.	0.
3	0.	0.2	0.
4	0.2	0.2	0.
5	0.1	0.1	0.1
6	0.	0.	0.2
7	0.2	0.	0.2
8	0.	0.2	0.2
9	0.2	0.2	0.2

	local minimum 1†			*idealized local minimum 1*¶		
atom number	*x (nm)*	*y (nm)*	*z (nm)*	*x (nm)*	*y (nm)*	*z (nm)*
1	0.208	0.419	0.242	0.	0.	0.
2	0.442	0.432	0.467	0.2	0.	0.2
3	0.216	0.116	0.235	0.	0.2	0.
4	0.412	0.116	0.245	0.2	0.2	0.
5	0.308	0.015	0.047	0.1	0.1	0.3
6	0.210	0.414	0.455	0.	0.	0.2
7	0.389	0.389	0.457	0.2	0.	0.2
8	0.214	0.109	0.453	0.	0.2	0.2
9	0.413	0.117	0.454	0.2	0.2	0.2

	local minimum 2†			*idealized local minimum 2*¶		
atom number	*x (nm)*	*y (nm)*	*z (nm)*	*x (nm)*	*y (nm)*	*z (nm)*
1	0.256	0.365	0.293	0.	0.	0.
2	0.260	0.086	0.488	0.	0.2	0.2
3	0.254	0.061	0.293	0.	0.2	0.
4	0.453	0.064	0.292	0.2	0.2	0.
5	0.360	0.478	0.403	0.1	0.1	0.1
6	0.250	0.358	0.499	0.	0.	0.2
7	0.457	0.364	0.496	0.2	0.	0.2
8	0.245	0.051	0.009	0.	0.2	0.2
9	0.459	0.069	0.069	0.2	0.2	0.2

† The conditions at which the local minima are obtained are described in the text.
¶ The idealization was obtained by taking nearest points within a centered-cube type arrangement (with taking the periodity of 0.5 nm into account) and shifting the centered cube to 0.1, 0.1, 0.1.

obtained by testing different cooling protocols. However, the optimization at 0.2 nm resolution gave a correct structure within 350 steps with a mean coordinate deviation of 0.01 nm. This reflects the fact that resolution reduction removed the existing energy barrier between the local and global energy minimum, Figure 3a vs. Figure 3b.

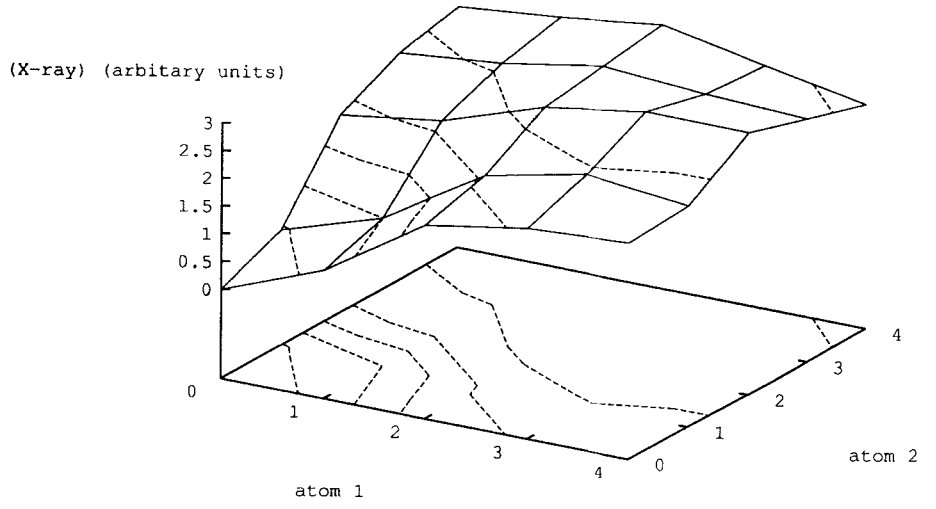

Figure 3a

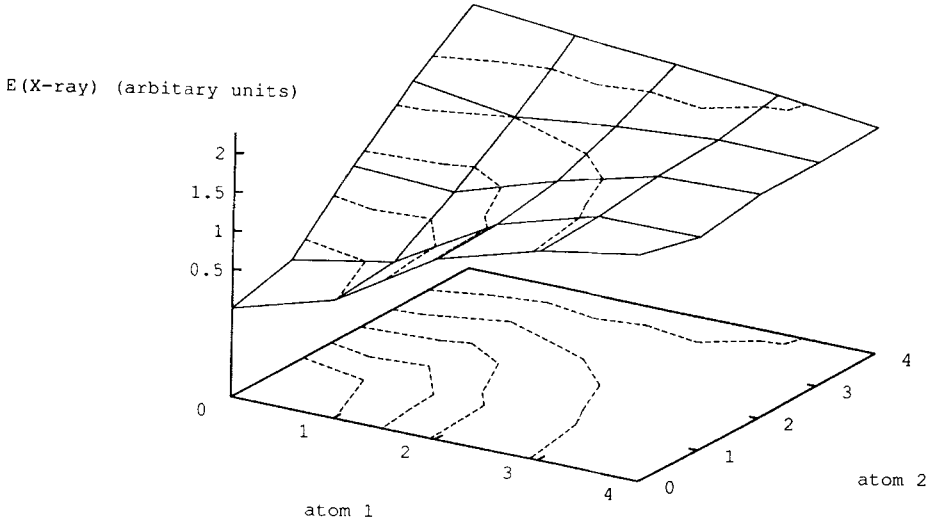

Figure 3b

c MD simulations with structure-factor averaging

The parameters that differ between conventional MD refinement and time averaging are the structure factor relaxation time τ_x and the atomic B-factors B_i. Conventional MD-refinement corresponds to $\tau_x = 0$ ps with optimized B_i's, whereas in time averaging τ_x has a positive finite value with strongly reduced B_i's. We examined the effects of various τ_x and B_i combinations, see Table 2. Clearly,

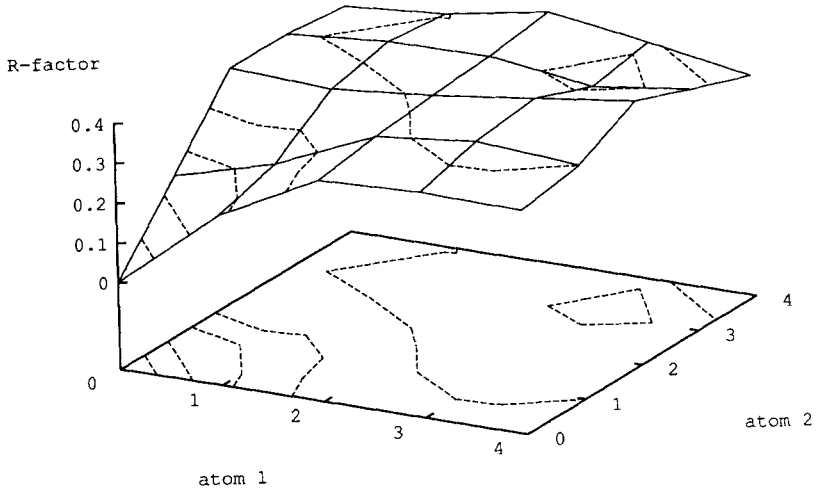

Figure 3c

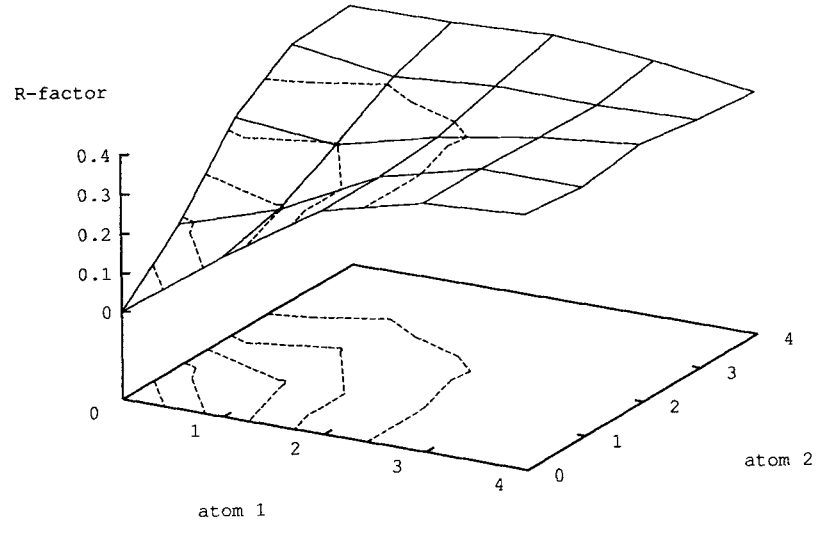

Figure 3 X-ray pseudo energy and R-factor as a function of atom positions. X-ray pseudo energies and R-factors were calculated for a set of structures in between the correctly centered cube configuration and local minimum 1 (see Table 1). The two deviating coordinates were each changed in 0.05 nm steps. Step 0 refers to the correct coordinate, whereas step 4 refers to 0.2 nm coordinate error. X-ray energy (see Equation 2) calculated using $w_x = ½\ k_x = 3.052\ 10^5$, and using data to (**a**) 0.1 nm resolution and (**b**) 0.2 nm resolution. Crystallographic R-factor for (**c**) data to 0.1 nm resolution and (**d**) data to 0.2 nm resolution. Dashed lines connect points with equal function values. The separation between these isolines is 0.5 10^5 kJ mol^{-1} I^{-1} (where I is an arbitrary unit for structure-factor intensities) for the X-ray pseudo energy and 0.067 for the crystallographic R-factor. The base plane contains a projection of these isolines.

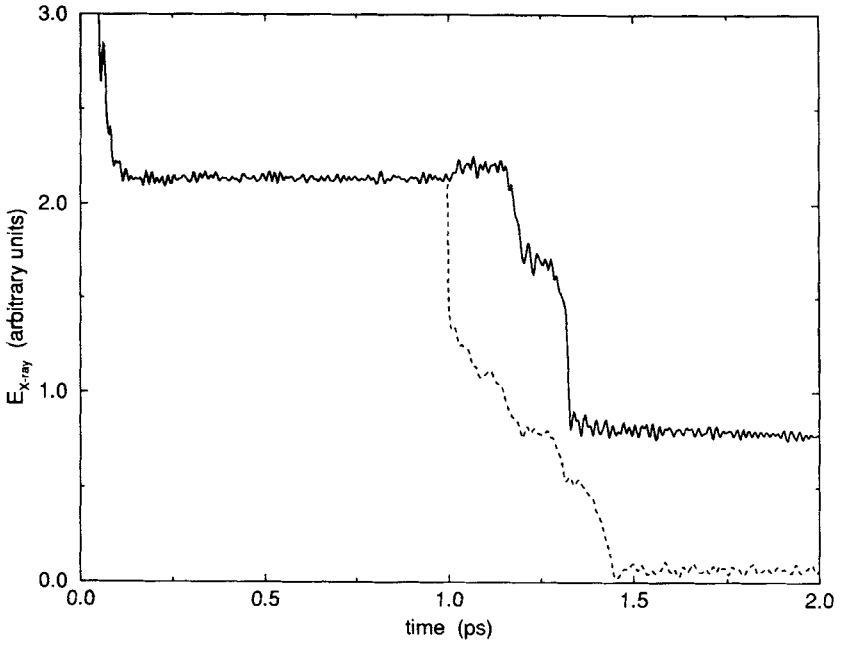

Figure 4 Simulated annealing and low-resolution MD-refinement starting in a local energy minimum. Local minimum 1 was obtained after 500 steps (1 ps) of MD-refinement at 300 K. This structure was further refined applying simulated annealing from 600 K down to 300 K over 500 steps. The structure was optimized against data to 0.1 nm resolution (248 reflections) (solid line). Starting from the same local minimum the structure was also refined against 0.2 nm resolution data (40 reflections) at 300 K (dashed line). The structure of local minimum 1 corresponded to an energy of 2.1 (10^5 kJ mol^{-1} I^{-1}, where I is an arbitrary structure-factor intensity unit); the local minimum obtained after simulated annealing (minimum number 2 in Table 1) was at $V_{X\text{-ray}} = 0.8$. Starting the simulated annealing at 900 K produced similar results to starting simulated annealing at 600 K. The energy at the start of the low-resolution refinement was 1.4 and dropped to 0.06. In a subsequent refinement at 300 K using 0.1 nm resolution data of this low-resolution solution the X-ray energy started at 0.2 and dropped quickly to 0.07. These calculations were performed with a weight factor of $w_x = 3.052\ 10^5$ and a structure-factor scale factor of $k = 1$.

correct B-factors of 0.10 nm^2 produced the best fit when $\tau_x = 0$ ps (see Table 2A). The R-factor of 5.14% in this case is due to positional variations caused by the kinetic energy in the simulation. Performing time-averaged sampling, using $\tau_x > 0$ ps, low R-factors are achieved when B_i is strongly reduced. Best R-factors were obtained for B-factors of 0.01 and 0.02 nm^2 and a τ_x of 10 ps. When applying time-averaging the atomic distributions are modelled by the ensemble of structures and the crystallographic B-factors have become obsolete.

In the original application of time averaging to crystallographic data we already noticed a significant heating during the simulation [11]. For conventional MD-refinement no heating is observed, see Table 2A. In the case of a finite relaxation time, $\tau_x > 0$ ps, the force field is non-conservative and leads to heating. The observed heating is inversely related to the relaxation time and the atomic B-factors (Table 2A). This observation can be explained by the fact, that the pseudo-energy function, $V_{X\text{-ray}}$ (see Equations (4) and (5)), imposes a complete sampling within a

time period related to τ_x of the distribution as represented by the structure-factor amplitudes. The use of small values for τ_x and B_i's reduces the sampling efficiency, hence leading to increased temperatures.

Besides the experiments with fixed 'perfect' scale factors, $k = 1$, we tested two schemes to optimize the scale factor, k, during the time-averaging simulation (see Table 2B). We updated the scale factor in an unrestrained manner, using Equation (3) where F_{calc} is replaced by the running average $\langle F_{calc} \rangle_t$, at 10, 100 and 500 step intervals; and, using Equation (7) with $\tau_k = 1$ ps, where the change in scale factor

Table 2 Variation of relaxation time, τ_x, and atomic B-factor, B, in time-averaging of crystallographic data.

A. Fixed 'perfect' scale factor, $k = 1$.[¶]

	R[§]				
B (nm^2)	0.01	0.02	0.05	0.10	0.20
τ_x (ps)					
0.	1.60	1.29	0.642	0.0514	0.498
1.	0.134	0.146	0.144	0.0689	0.340
5.	0.0653	0.0684	0.0716	0.113	0.326
10.	0.0420	0.0394	0.0657	0.114	0.362

	$\langle T \rangle$ (K)[‡]				
B (nm^2)	0.01	0.02	0.05	0.10	0.20
τ_x (ps)					
0.	280.6	287.5	293.1	293.8	296.8
1.	2568.	2465.	1343.	484.6	438.4
5.	839.7	746.5	650.1	438.0	323.3
10.	583.3	542.8	485.1	401.1	309.1

B. Updating of the scale factor; $\tau_x = 5$ ps[†].

	R[§]				
B (nm^2)	0.01	0.02	0.05	0.10	0.20
scaling parameters					
$\tau_k = 0$ ps, $\Delta n = 10$	0.0874	0.0868	0.0721	0.0723	0.0424
$\tau_k = 0$ ps, $\Delta n = 100$	0.0766	0.0672	0.0610	0.0720	0.0660
$\tau_k = 0$ ps, $\Delta n = \infty$	0.0653	0.0684	0.0716	0.113	0.326
$\tau_k = 1$ ps, $\Delta n = 1$	0.0505	0.0618	0.0636	0.102	0.255

	scale factor, k[¿]				
B (nm^2)	0.01	0.02	0.05	0.10	0.20
scaling parameters					
$\tau_k = 0$ ps, $\Delta n = 10$	2.13	2.27	2.05	2.42	2.64
$\tau_k = 0$ ps, $\Delta n = 100$	1.62	1.58	1.70	1.63	2.38
$\tau_k = 0$ ps, $\Delta n = \infty$	1.	1.	1.	1.	1.
$\tau_k = 1$ ps, $\Delta n = 1$	1.09	1.09	1.10	1.13	1.25

		$\langle T \rangle$ (K)¡				
	B (nm^2)	0.01	0.02	0.05	0.10	0.20
scaling parameters						
τ_k = 0 ps, Δn = 10		1096.	1054.	722.9	666.4	524.9
τ_k = 0 ps, Δn = 100		1069.	954.5	745.3	587.9	486.7
τ_k = 0 ps, Δn = ∞		839.7	746.5	650.1	438.0	323.3
τ_k = 1 ps, Δn = 1		928.4	774.4	585.1	517.4	345.5

¶ The simulation time was 1, 1, 5, and 10 ps for experiments with τ_k = 0, 1, 5 and 10 ps respectively using a weight factor of $w_x = 3.052\ 10^5$.
§ The R-factors are calculated using the running-average structure factors obtained at the end of the simulation. In case of τ_x = 0 ps, the running-average structure factors correspond to the instantaneous structure factors.
¡ The temperatures correspond to the average temperature over the whole simulation.
† Simulation length for these experiments was 5 ps. The scaling of $|\langle F_{calc} \rangle_t|$ to $|F_{obs}|$ was performed in 4 different ways: a. updating the scale factor (every 10 time steps (Δt = 2 fs), indicated by τ_k = 0 ps, Δn = 10; b. updating the scale factor every 100 steps, τ_k = 0 ps, Δn = 100; c. fixed scaling, where the scale factor of was kept at the value 1 throughout the simulation, τ_k = 0 ps, Δn = ∞; and, d. updating the scale factor every step, but assigning a relaxation time of τ_k (see Equation (7)), τ_k = 1 ps, Δn = 1.
¿ The scale factors given are obtained at the end of the simulation.

is dampened over time. The scale factor increased in all these experiments, and no convergence could be observed. The smallest deviation was observed for the dampened time-dependent scale factor, $\langle k \rangle_t$ (Equation (7)), where the scale factor was 1.09 after 5 ps (1.19 after 10 ps). Applying the unrestrained updating every 500 steps (every 1 ps) produced a scale factor of 1.12 after 5 ps, indicating the similarity to the time-dependent update experiment with τ_k = 1 ps. Since the particles have no physical interaction (V_{phys} = 0) in the presented experiments, their probability distribution is absolutely flat in the absence of the X-ray restraint. Allowing the scale factor to be updated when V_{phys} = 0, favors the flat distribution where the X-ray data is modelled by ever decreasing fluctuations in the distribution.

Three ensembles were collected at different relaxation times, τ_x = 2.5, 5 and 10 ps with $B_i = 0.01$ nm^2 using data to 0.1 nm resolution, a scale factor of k = 1, and a weight factor of $w_x = 3.052\ 10^5$. In these cases we employed equilibration scheme II. Due to the fact that τ_x = 0 at t = 0 ps, the influence of starting at a perfect solution may be regarded as negligible. This is illustrated by the R-factor rising to relatively large values (above 30%) in the early stages of this type of equilibration. Figure 5 shows the trajectory of the 9 atoms as obtained in the simulation with τ_x = 5 ps over 50 ps of simulation after 30 ps equilibration. Many cross-overs from peak to peak are observed in Figure 5a. This reflects the extreme condition under which these experiments were performed, V_{phys} = 0. Since all particles are identical in our simulation and have no physical interaction, any position can be sampled by any particle at any time. More particles may even sample one peak at the same time. The scatter representation of the trajectory (Figure 5b) clearly shows that the centered cube configuration is reproduced, with peak maxima at correct distances. The overall R-factors that are obtained for the ensemble models collected at τ_x = 2.5, 5 and 10 ps are 7.9%, 3.8% and 3.1% respectively. The R-factors as they appear during the simulation, i.e. that correspond to the running average structure factors, are about twice as large. Figure 6 depicts the fluctuations in $V_{X\text{-ray}}$ as observed during the ensemble-collection period.

The number of parameters in an ensemble description is obviously much larger than in a conventional single-structure model. In view of the fact that only structure-factor amplitude information is used, the various ensembles of structures collected

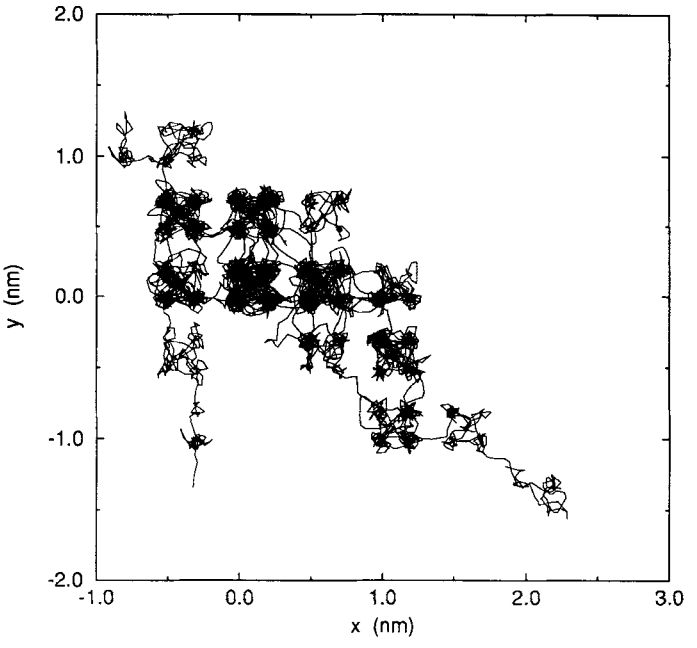

Figure 5a

at 0.1 nm resolution data (248 reflections) are surprisingly good. Reducing the number of observations to 40 reflections, i.e. data to 0.2 nm resolution, yielded ensembles with good R-factors (running R-factors around 5%) for $\tau_x = 1$ and 5 ps and $B_i = 0.01\,\text{nm}^2$, but the structural features of the centered cube were completely lost (see Figure 7). A similar answer was obtained when the time-averaging simulation was started from random atom positions using data to 0.1 nm resolution. This indicates that the system got trapped in a local energy minimum, that has essentially the same features as an underdetermined low resolution ensemble.

An important potential disadvantage of time-averaging is its potency to sample noise present in the structure-factor amplitudes. We studied this aspect by introducing noise to the 'observed' structure-factor amplitudes. The R-factor between this new data set and the perfect data set was 9.3%. Refining the positional parameters of the conventional model (again with perfect B_i's of $0.10\,\text{nm}^2$) against the noisy data resulted in a R-factor of 8.6%. Time-averaging simulations on this noisy data were performed with relaxation times of $\tau_x = 5$ and 10 ps with $B_i = 0.01\,\text{nm}^2$, $k = 1$, $T_{\text{bath}} = 300\,\text{K}$ and $w_x = 3.052\ 10^5$. In both cases the R-factors of the ensemble were higher than for the ensemble determined with perfect data, but also lower than 9.3%, see Table 3. The situation becomes only slightly worse (less than 1%) when the relaxation time is increased from 5 ps to 10 ps. Clearly, some but not all aspects of the noise in the data have been sampled and are represented by the structures in the ensemble. In the simulations no discrimination was made between perfect data and noise that correlates with mere distortions of positive electron density. We should, therefore, expect these effects to be represented in the collected ensemble. The only constraint active in the presented test experiments was that the data had to correspond to positive electron density. Noise that conflicts this

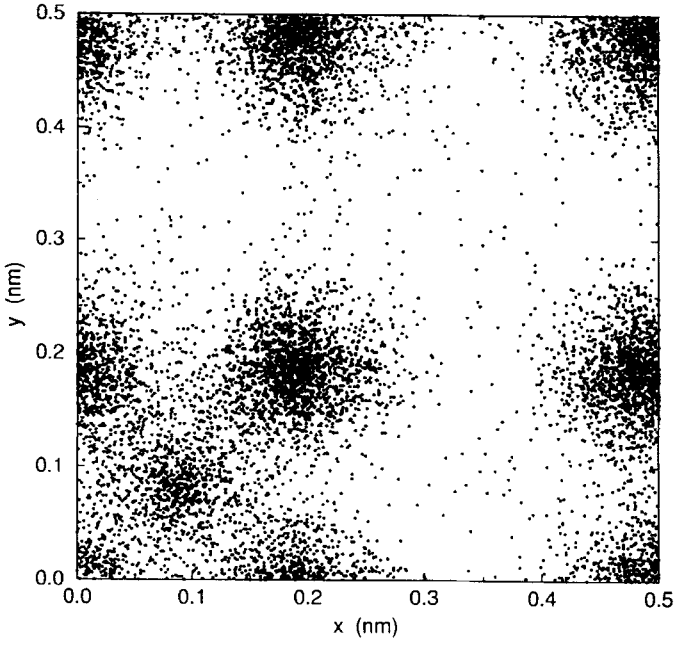

Figure 5 Time-averaging trajectory of the 9 atoms collected at 0.1 nm resolution. Trajectories of 9 atoms recorded in a time-averaging simulation with $\tau_x = 5$ ps, $B_i = 0.01$ nm^2 at 0.1 nm resolution and with $T_{bath} = 300$ K, $k = 1$, and $w_x = \frac{1}{2} k_x = 3.052\ 10^5$. **(a)** The xy-plane projection of the trajectories of all 9 atoms, **(b)** scatter representation of the trajectories projected onto one unit cell. Every dot represents one atomic position in the trajectory of the 9 atoms. The coordinates were collected every 25 steps (50 fs) during the ensemble collection period of 50 ps after 30 ps equilibration.

positivity restraint is, therefore, not represented in the ensemble-average structure factor set.

5. CONCLUSIONS

The presented test system of 9 atoms turned out to be stable in a conventional MD-refinement using only its 28 lowest resolution reflection intensities. In our application, the 27 positional coordinates were the only independent variables. The functional form and the width of the atomic density were taken as a constraint. Starting from random coordinates, the system refined to a correct centered-cube configuration. It was shown, that high resolution data introduced local energy minima in the X-ray pseudo-energy function. As a consequence, *ab initio* refinement converged faster at low resolution, after which the resolution could be extended to obtain a more precise answer.

The time-averaging experiments on the 9 atom system were performed under the same condition of having no physical force field ($V_{phys} = 0$) in the calculations. Furthermore, in contrast to the conventional MD-refinement, no constraints or restraints were present for the functional form and width of the atomic

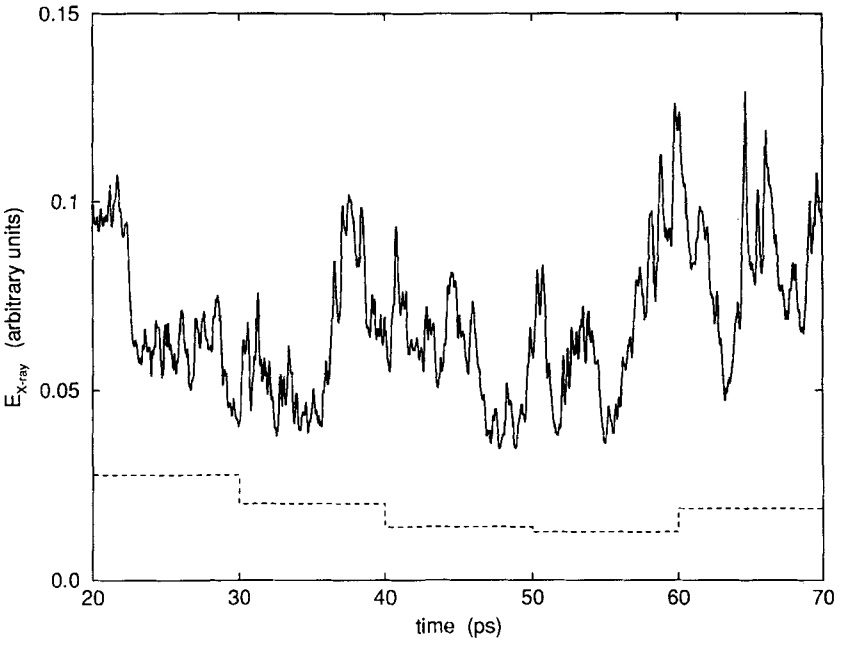

Figure 6 X-ray pseudo energy during a time-averaging simulation. The X-ray energies (see Equation (4)) of the simulation at $\tau_x = 5$ ps are shown. The energies (in 10^5 kJ mol^{-1} I^{-1}, where I is an arbitrary unit for structure factor intensities) computed from the running average of the calculated structure factors, as they appear at the stage of collecting the ensemble, are shown in solid lines. The dashed line depicts the X-ray energy of the cumulative average structure factors. This averaging is performed in blocks of 10 ps. T_{bath}, k, and w_x values as in Figure 5.

electron-density distributions. In that sense, time-averaging was applied under extreme demanding circumstances.

A correct ensemble, representing a centered-cube configuration, was obtained using only X-ray data to 0.1 nm resolution (248 reflections), that is without applying any physical force field. Best results with R-factors around 3 to 4% were obtained at this resolution, when the sampling time was extended to 5 or 10 ps. Reduction to 0.2 nm resolution (40 reflections) resulted in underdetermination of the number of parameters versus the number of observables. The structure-factor scale factor increased continuously when optimized in a time-averaged restrained simulation. This is caused by the fact that an uniform density distribution would be obtained in the absence of the crystallographic pseudo-energy function for these experiments where $V_{phys} = 0$.

It appeared that not all noise was sampled and represented by the time-averaging technique. In essence, noise is indistinguishable from real data if no information in the form of restraints or constraints are applied. The technique of time-averaged restraint MD simulation will sample the conformations, given all constraints and restraints that have been defined, weighted according to the Boltzmann factor ($\exp[-V_{pot}/k_B T]$).

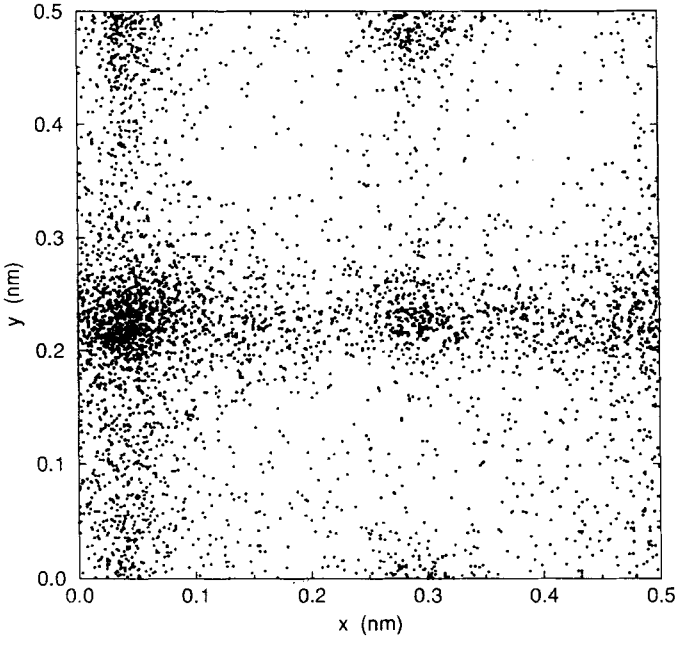

Figure 7 A time-averaging trajectory for a case with insufficient structure-factor-amplitude restraints. Scatter representation of a 50 ps trajectory of 9 atoms collected in a time-averaging simulation at 0.2 nm resolution with $\tau_x = 5$ ps and $B_i = 0.01$ nm^2. The trajectory was collected over a period of 50 ps after 30 ps equilibration at intervals of 50 fs. Each dot represents one position in the trajectory. T_{bath}, k, and w_x values as in Figure 5.

Table 3 Effects of noise in time-averaging simulations.

	R-factor¶	
	perfect data	*noisy data*§
$\tau_x = 5$ ps	0.038	0.055 (0.077)
$\tau_x = 10$ ps	0.031	0.049 (0.085)

¶ The given R-factors are calculated from the ensemble averaged structure factors and the 'observed' structure factor amplitudes as used in the simulation, i.e. using perfect data and noisy data as indicated.

§ The R-factors given in parentheses are R-factors against the perfect structure factor amplitudes, while the ensemble averaged structure factors were computed from a simulation against noisy data.

These simulations were performed with a bath temperature of $T_{bath} = 300$ K, a scale factor of $k = 1$, and a weight factor of $w_x = 3.052\ 10^5$.

Acknowledgements

It is a pleasure to thank Dr C.A. Schiffer for stimulating discussions and reading the manuscript.

References

[1] W.F. van Gunsteren, R. Kaptein and E.R.P. Zuiderweg, "Use of Molecular Dynamics Computer Simulations when Determining Protein Structure by 2D NMR", in *Proc. NATO/CECAM workshop on nucleic acid conformation and dynamics*, W.K. Olson ed., CECAM, Orsay, France (1984), 79–92.

[2] R. Kaptein, E.R.P. Zuiderweg, R.M. Scheek, R. Boelens and W.F. van Gunsteren, "A Protein Structure from Nuclear Magnetic Resonance Data *lac* Repressor Headpiece", *J. Mol. Biol.*, **182**, 179–182 (1985).

[3] G.M. Clore, A.M. Gronenborn, A.T. Brünger and M. Karplus, Solution Conformation of a Heptadecapeptide Comprising the DNA Binding Helix F of the Cyclic AMP Receptor Protein of *Escherichia coli*", *J. Mol. Biol.* **186**, 435–455 (1985).

[4] A.T. Brünger, J. Kuriyan and M. Karplus, "Crystallographic R Factor Refinement by Molecular Dynamics", *Science* **235**, 458–460 (1987).

[5] A.T. Brünger, "Crystallographic Refinement by Simulated Annealing, Application to a 2.8 Å Resolution Structure of Aspartate Aminotransferase", *J. Mol. Biol.*, **203**, 803–816 (1988).

[6] M. Fujinaga, P. Gros and W.F. van Gunsteren, "Testing the Method of Crystallographic Refinement Using Molecular Dynamics", *J. Appl. Cryst.*, **22**, 1–8 (1989).

[7] J.L. Smith, W.A. Hendrickson, R.B. Honzatko and S. Sheriff, "Structural Heterogeneity in Protein Crystals", *Biochemistry*, **25**, 5018–5027 (1986).

[8] J. Kuriyan, G.A. Petsko, R.M. Levy and M. Karplus, "Effect of Anisotropy and Anharmonicity on Protein Crystallographic Refinement, An Evaluation by Molecular Dynamics", *J. Mol. Biol.*, **190**, 227–254 (1986).

[9] W.F. van Gunsteren and H.J.C. Berendsen, "Computer Simulation of Molecular Dynamics: Methodology, Applications and Perspectives in Chemistry", *Angew. Chem. Int. Ed. Engl.*, **29**, 992–1023 (1990).

[10] A.E. Torda, R.M. Scheek and W.F. van Gunsteren, "Time-averaged Nuclear Overhauser Effect Distance Restraints Applied to Tendamistat", *J. Mol. Biol.*, **214**, 223–235 (1990).

[11] P. Gros, W.F. van Gunsteren and W.G.J. Hol, "Inclusion of Thermal Motion in Crystallographic Structures by Restrained Molecular Dynamics", *Science*, **249**, 1149–1152 (1990).

[12] A.E. Torda, R.M. Scheek and W.F. van Gunsteren, "Time-Dependent Distance Restraints in Molecular Dynamics Simulations", *Chem. Phys. Lett.*, **157**, 289–294 (1989).

[13] D.A. Pearlman and P.A. Kollman, "Are Time-averaged Restraints Necessary for Nuclear Magnetic Resonance Refinement", *J. Mol. Biol.*, **220**, 457–479 (1991).

[14] A. Pastore, V. Saudek, G. Ramponi and R.J.P. Williams, "Three-Dimensional Structure of Acylphosphatase, Refinement and Structure Analysis", *J. Mol. Biol.*, **224**, 427–440 (1992).

[15] M.A. Castiglione Morelli, A. Pastore and A. Motta, "Dynamic Properties of Salmon Calcitonin Bound to Sodium Dodecyl Sulfate Micelles: A Restrained Molecular Dynamics Study from NMR Data", *J. Biomolecular NMR*, **2**, 335–348, (1992).

[16] A.E. Torda, R.M. Brunne, T. Huber, H. Kessler and W.F. van Gunsteren, "Structure Refinement using Time-Averaged J-Coupling Constant Restraints", *J. Biomolecular NMR*, accepted for publication.

[17] P. Gros, "Time-Averaged Crystallographically Restrained Molecular Dynamics", in *Crystallographic Computing 5, From Chemistry to Biology*, D. Moras, A.D. Podjarny and J.C. Thierry, eds. Int. Union of Cryst., Oxford University Press, 1991, ch. 31.

[18] W.F. van Gunsteren and H.J.C Berendsen, *Groningen Molecular Simulation (GROMOS) Library Manual* (1987), Biomos, Groningen, The Netherlands.

[19] R.C. Agarwal, "A New Least-Squares Refinement Technique Based on the Fast Fourier Transform Algorithm", *Acta Cryst.*, **A34**, 791–809 (1978).

[20] R.C. Agarwal, "New Results on Fast Fourier Least-Squares Refinement Technique", in *Refinement of Protein Structures*, P.A. Machin, J.W. Campbell and M. Elder eds., Proc. Daresbury Study Weekend (1980), ch. 4.

[21] H.J.C. Berendsen, J.P.M. Postma, W.F. van Gunsteren, A. Dinola and J.R. Haak, "Molecular Dynamics with Coupling to an External Bath", *J. Chem. Phys.*, **81**, 3684–3690 (1984).

[22] A.T. Brünger, M. Karplus & G.A. Petsko, "Crystallographic Refinement by Simulated Annealing: Application to Crambin", *Acta Cryst.* **A45**, 50–61 (1989).

[23] P. Gros, M. Fujinaga, B.W. Dijkstra, K.H. Kalk and W.G.J. Hol, "Crystallographic Refinement by Incorporation of Molecular Dynamics: Thermostable Serine Protease Thermitase Complexed with Eglin c", *Acta Cryst.*, **B45**, 488–499, (1989).